

05.1

Impact loading of laminated composites ZrO_2/Ti and ZrO_2/Al with non-rigid interfaces

© Yu.F. Gomorova¹, S.P. Buyakova¹, A.G. Burlachenko¹, A.S. Buyakov¹, A.E. Kuznetsova¹, Yu.V. Dontsov²

¹ Institute of Strength Physics and Materials Science, Siberian Branch, Russian Academy of Sciences, Tomsk, Russia

² Tomsk Polytechnic University, Tomsk, Russia

E-mail: gomjf@ispms.ru

Received January 9, 2023

Revised March 10, 2023

Accepted March 10, 2023

The article presents the results of studying the impact response of ceramic-metal composites ZrO_2/Ti and ZrO_2/Al with non-rigid fixing of layers. It is shown that, as the energy dissipates from layer to layer, there takes place an increase in the dispersion of the structure of metal foils and ceramic plates. The ZrO_2/Ti ceramic-metal composites have a higher impact strength, while the impact strength of layered ZrO_2/Al composites differs from the impact strength of monolithic ceramics only scarcely. It was shown that, regardless of the distance between the ceramic plates and the point of impact, their destruction occurs with the transformation of the ZrO_2 tetragonal modification into the monoclinic one.

Keywords: layered ceramic-metal composites, impact strength.

DOI: 10.21883/TPL.2023.05.56022.19501

Dispersion-reinforced composites with a metal or ceramic matrix have found wide application in many fields of engineering. Their response to external mechanical impacts has been well studied by many researchers. In such composites, mainly one of the phases is continuous. In composites with the ceramic matrix and metallic inclusions, the ceramic matrix ensures high strength, while the influence of the metallic phase manifests itself as an increase in the fracture toughness of the composite as a whole [1–4].

For composites with continuous metal and ceramic phases to which layered-structure composite materials belong, the response to mechanical impact is less studied. Depending on the intended practical application of the layered composites, one of their phases (ceramic or metallic) may be predominant. In view of practical application, composites having structures consisting of ceramic and metal layers are of interest for electronics, engine engineering, missile industry, aircraft industry [5–9]. The incentive for developing and studying properties of layered ceramic-metal materials is the necessity of combining in the material a rigidity exceeding that of metals and failure toughness exceeding that of single-phase ceramics.

This work is devoted to studying impact-load-induced destructions of composites consisting of alternating metal and ceramic layers. Thickness of ceramic layers in the composites under study exceeded essentially that of metal layers. Along with this, composites had no rigid interfaces between the metal and ceramic layers; the layers were attached to each other with glue, hence, after removing the glue it became possible to analyze impact-induced modifications of the layer surfaces.

Fig. 1, *a* presents a schematic structure of metal-ceramic composites obtained in this study. The composites consisted of alternating ceramic plates 2 mm thick and metal foils 100 μm thick attached to each other with a cyanoacrylate adhesive.

Ceramics used in the composites obtained here was based on zirconium dioxide ZrO_2 stabilized with 3 mol.% yttrium oxide Y_2O_3 . The ceramics phase composition was represented by the ZrO_2 tetragonal modification. The ceramic components of the layered composites were obtained by molding the ZrO_2 powder. Relative density of the composites ceramic layers was $97.8 \pm 0.2\%$. For the purpose of studying, there were also prepared ceramic samples whose geometry was the same as that of the composites ceramic layers.

The obtained layered composites differed from each other in metal layers. Some composites comprised titanium foil VT1-0, in other ones aluminum foil A999 was used. The metal foils were fabricated by rolling to the thickness of 300 μm followed by annealing during an hour (at 800°C for Ti foils, 300°C for Al foils). The obtained foils were thickened-out to 100 μm by electrolytic polishing.

Mechanical tests were performed at room temperature using a pendulum impact tester with the console-fixed sample on testing machine Gotech GT-7045 H. In the experiment, impact strength a_n [J/cm^2] was determined via the ratio of the energy spent on deforming and destructing the samples to the area of the sample cross-section at the point of impact. The test scheme is presented in Fig. 1, *b*. The impact was made on the side of the ceramic layer (*Frontal surface*). The striker energy was 15 J, the motion speed was 3.46 m/s. After subjecting the composites to

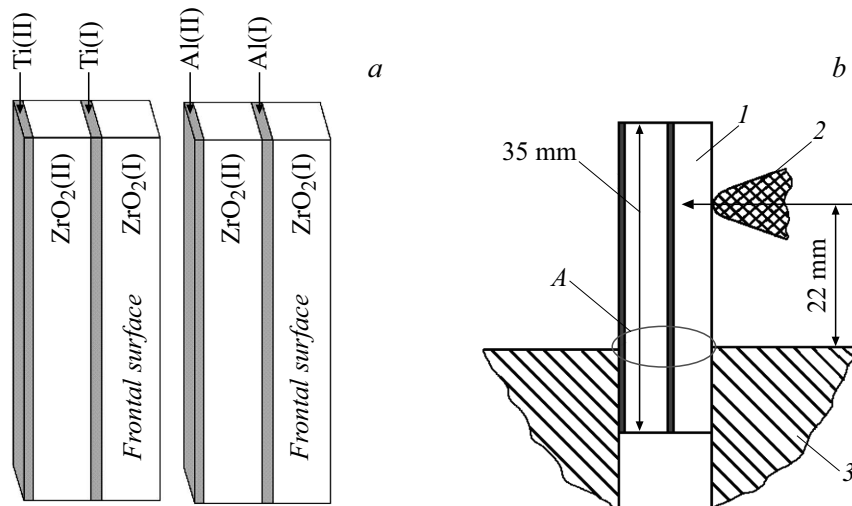


Figure 1. *a* — schematic structure of layered ceramic-metal composites. *b* — scheme of the impact-bending test. *1* — sample, *2* — striker of the pendulum impact tester, *3* — clamp. *A* — area of post-testing structural and phase investigations.

impact loading, the adhesive was dissolved. The released composite layers were studied in region *A* indicated in Fig. 1, *b*.

X-ray structural analysis was performed based on diffraction patterns obtained using a diffractometer with filtered $\text{CoK}\alpha$ radiation. Dimensions of the phase-coherent scattering areas (CSA) were determined via the Scherrer equation [10], while magnitudes of cell micro-distortion were obtained via the Wilson-Stokes formula [11]. Amount of the zirconium oxide monoclinic phase was calculated by the Rietveld method [12]. The composite structure was studied by the methods of optical microscopy (Altami MET) and scanning electron microscopy (SEM) (Vega Tescan).

Prior to impact loading of the composite, the Ti foil consisted of polyhedral equiaxed grains $45 \pm 6 \mu\text{m}$ in size. The Al foil initial structure was represented by equiaxed grains with the mean size of $71 \pm 12 \mu\text{m}$.

The results of mechanical tests showed that the impact strength of layered composite ZrO_2/Ti was higher than those of ceramics $\text{ZrO}_2(\text{Y}_2\text{O}_3)$ and composite ZrO_2/Al . Impact strength of the ZrO_2/Ti composite samples was in average $a_n = 2.95 \text{ J/cm}^2$, mean impact strength of the $\text{ZrO}_2(\text{Y}_2\text{O}_3)$ samples was 1.10 J/cm^2 . The presence of aluminum foil layers in the ZrO_2/Al layered composite did not significantly affect quantity a_n whose mean value for the composite samples was $a_n = 1.12 \text{ J/cm}^2$. Such a significant difference between the values of impact strength of layered ceramic-metal composites ZrO_2/Ti and ZrO_2/Al is caused by the difference in Ti and Al strength characteristics; the titanium VT1-0 ultimate strength (σ_B) is 375 MPa, while that of aluminum A999 is only 59 MPa.

The impact effect is most harmful in view of reliability and durability of ceramic ware and structural components. Ceramic plates of the ZrO_2/Ti and ZrO_2/Al composites got

destroyed under the impact regardless of the distance from the striker application point.

Titanium foils in the samples of layered composite ZrO_2/Ti were significantly deformed in the region of impact, but retain their integrity. Fig. 2, *a, b* presents SEM images of the Ti(I) and Ti(II) foil surfaces. On the Ti(I) foil located closer to the impact front, a neck was formed at the place of bending (Fig. 2, *a*). Grain sliding in both foils is mainly solitary. The Ti(I) foil photos show that in the formed neck a grain deformation is clearly visible in the direction of tensile strain (inset in Fig. 2, *a*). The Ti(II) foil deformation pattern exhibits lower extent of development than the Ti(I) foil pattern, which stems from the impact energy dissipation during destruction of the second ceramic layer (inset in Fig. 2, *b*).

X-ray diffraction analysis of titanium foils showed that the mean CSA size of the Ti(I) foil was 49.1 nm, while that of the Ti(II) foil was 62.1 nm. In the initial state, the CSA size of the first and second foils was 85.7 nm. The difference in the foil CSA sizes prior to and after impact loading evidences for the blocks' dispersion due to plastic deformation and also for formation of new sub-boundaries in the foils. Dispersion in the Ti(I) foil located closer to the impact front was more intense. The Ti(I) and Ti(II) foils differed also in magnitudes of micro-distortions of elementary cells: $\varepsilon = 0.0012$ for the Ti(I) foil and $\varepsilon = 0.00092$ for the Ti(II) foil which is more distant from the impact point.

In the process of impact loading of composite ZrO_2/Al , all the ceramic layers, as well as one of the metal layers, were fully destroyed. Foil Al(I) was fully broken, foil Al(II) was partially destroyed. Fig. 2, *c* presents the foil Al(I) structure. Based on the photo, it is possible to conclude that the destruction is of the quasi-viscous character (inset in Fig. 2, *c*), which is caused by the material subdivision into lamellas during the main crack propagation over the

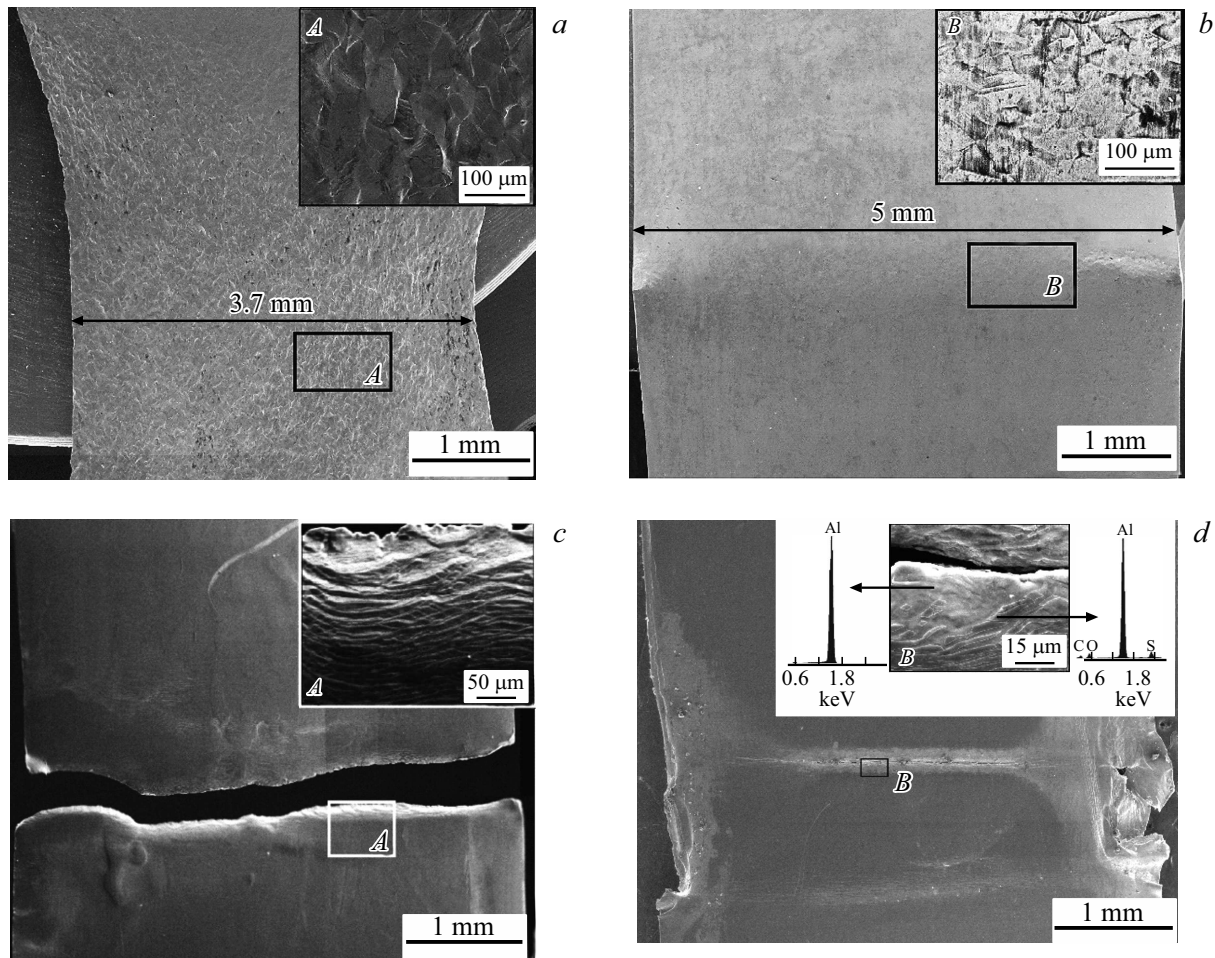


Figure 2. SEM images of the deformation pattern of the foil surface. *a, b* — composite ZrO_2/Ti : foil Ti(I) (*a*) and foil Ti(II) (*b*); *c, d* — composite ZrO_2/Al : foil Al(I) (*c*) and foil Al(II) (*d*).

area of localized striker-induced deformation. Foil Al(II) has undergone partial destruction. As Fig. 2, *d* shows, the main crack emerged but did not result in total destruction.

The presence of the Al_2O_3 oxide films on the aluminum foil surfaces led to their multiple cracking and delamination in the area of foil deformation and destruction (inset in Fig. 2, *d*), since the state of material along the crack edges is strongly nonequilibrium. The elemental analysis revealed the presence of oxygen, sulfur and carbon only in the fragile film. The presence of sulfur and carbon is caused by their accumulation on the foil surface in the process of electrolytic polishing.

X-ray diffraction analysis of aluminum foils demonstrated reduction of CSA relative to the initial value. For instance, initial CSA for the Al foils was 81.2 nm. After the impact loading, the mean CSA size in the Al(I) foil destruction area was 43.2 nm, that in the Al(II) foil in the area of the crack formation was 62.7 nm. The Al(I) and Al(II) foils differed also in magnitudes of elementary cell micro-distortions. The cell micro-distortion magnitude for the Al(I) foil was $\varepsilon = 0.0021$, that for the Al(II) foil was $\varepsilon = 0.0011$.

We have analyzed phase composition of the destruction surface of the ZrO_2 (I) and (II) ceramic layers for samples of both composites. A distinctive feature of the ceramics based on tetragonal zirconium dioxide is transformation-induced hardening resulting from martensitic transformation of tetragonal modification $t-ZrO_2$ to monoclinic one $m-ZrO_2$. The ZrO_2 tetragonal-monoclinic transformation proceeds in the front zone of the crack with considerable energy absorption, which provides a higher fracture toughness of the zirconium ceramics relative to those of ceramics of other types. The increment of monoclinic modification $m-ZrO_2$ on the destruction surface evidences for occurrence in ZrO_2 of martensitic transformation $t \rightarrow m$.

As per the results of X-ray diffraction analysis, prior to impact loading the ceramics composition included only the tetragonal phase of ZrO_2 . After testing, the content of ZrO_2 monoclinic phase in layer (I) of the ZrO_2/Ti composite samples appeared to be $\sim 37\%$ which is somewhat higher than in layer (II) ($\sim 34\%$). This evidences that the impact energy is absorbed in the titanium foil layer. The ZrO_2/Al composites did not exhibit the difference between the

monoclinic phase contents on the destruction surfaces of ceramic layers (I) and (II).

The obtained results allow us to make the following conclusions.

1. Impact tests showed that, among the tested ceramic-metal layered composites, the highest impact strength is possessed by composite ZrO₂/Ti in which the a_n value was 2.95 J/cm². Impact strength of the ZrO₂/Ti composite samples was $a_n = 1.12.95$ J/cm², which is comparable with the mean impact strength (1.10 J/cm²) of the ZrO₂(Y₂O₃) samples.

2. Under the impact loading of composite ZrO₂/Ti, the Ti foils remained intact while the sample as a whole was considerably deformed. In testing the ZrO₂/Al composite, the first Al foil located behind the front ceramic layer was fully destructed, while in the second Al foil fixed at the sample rear side a crack emerged but did not result in total destruction of the foil.

3. X-ray diffraction analysis of the ceramic plates revealed a higher content of the monoclinic phase in ZrO₂ in ceramic layers (I) and (II), which evidences for realization of the martensitic transformation $t \rightarrow m$ in ZrO₂.

Financial support

The study was carried out in the framework of State Assignment to ISPMS RAS SB (project FWRW-2021-0009).

Conflict of interests

The authors declare that they have no conflict of interests.

References

- [1] K. Konopka, M. Maj, K.J. Kurzydowski, *Mater. Character.*, **51**, 335 (2003). DOI: 10.1016/j.matchar.2004.02.002
- [2] P. Piotrkiewicz, J. Zygmuntowicz, M. Wachowski, K. Cymerman, W. Kaszuwara, *Materials*, **15**, 1848 (2022). DOI: 10.3390/ma15051848
- [3] J.J. Song, Y.S. Zhang, H.Z. Fan, Y. Fang, L.T. Hu, *Mater. Des.*, **65**, 1205 (2015). DOI: 10.1016/j.matdes.2014.09.084
- [4] Y. Wang, M. Li, H. Wang, G. Shao, J. Zhu, W. Liu, H. Wang, B. Fan, H. Xu, H. Lu, R. Zhang, *Metals*, **11**, 2018 (2021). DOI: 10.3390/met11122018
- [5] J. Park, S. Cho, H. Kwon, *Sci. Rep.*, **8**, 17852 (2018). DOI: 10.1038/s41598-018-36270-x
- [6] X.Q. Cao, R. Vassen, F. Tietz, D. Stoeber, *J. Eur. Ceram. Soc.*, **26**, 247 (2006). DOI: 10.1016/j.jeurceramsoc.2004.11.007
- [7] Y. Xing, S. Baumann, S. Uhlenbruck, M. Rüttinger, A. Venskutonis, W.A. Meulenbergh, D. Stöver, *J. Eur. Ceram. Soc.*, **33**, 287 (2013). DOI: 10.1016/j.jeurceramsoc.2012.08.025
- [8] S.Q. Guo, Y. Kagawa, T. Nishimura, H. Tanaka, *Ceram. Int.*, **34**, 1811 (2008). DOI: 10.1016/j.jeurceramsoc.2007.08.009
- [9] M.M. Opeka, I.G. Talmy, J.A. Zaykoski, *J. Mater. Sci.*, **39**, 5887 (2004). DOI: 10.1023/B:JMSS.0000041686.21788.77
- [10] P. Scherrer, in *Kolloidchemie* (Springer, Berlin–Heidelberg, 1912), p. 387. DOI: 10.1007/978-3-662-33915-2_7
- [11] A.R. Stokes, A.J.C. Wilson, *Proc. Phys. Soc.*, **56**, 174 (1944). DOI: 10.1088/0959-5309/56/3/303

- [12] C.J. Howard, R.J. Hill, *J. Mater. Sci.*, **26**, 127 (1991). DOI: 10.1007/BF00576042

Translated by Solonitsyna Anna